



# Integrated Data Analysis for Characterization of Fractured Basement Reservoir in Cambay Basin, India

Harsha Raghuvanshi<sup>1</sup>, B. Agrawal, S. P. Maurya, Debashree Paul, A. K. Paswan, V. K. Shukla, Kiran Sharma.

<sup>1</sup>Email: raghuvanshi\_harsha@ongc.co.in, Oil and Natural Gas Corporation Limited

## Abstract

The present study deals with basaltic traps (Deccan Traps) in the western onshore basin of India. The Deccan Trap is megascopically characterized by basaltic rock, which is divisible into four-five litho-units viz fresh, altered, weathered and amygdaloidal. Some of the basalt flows are vesicular. Vesicles are generally concentrated on the top of the trap flow regime. These vesicles, when fractured, form the best porosity zones. Subsequent mineralization and infilling of sediments in these fracture networks provide a porous and permeable space to the basement. Connectivity of fractured basement reservoir also depends upon the secondary clay mineralization within the fractures, which may play a dominant role in obstructing hydrodynamic connectivity. These highly weathered and fractured basalts form unconventional reservoir and they are the primary target for hydrocarbon exploitation. But, due to its complexities, the characterization of fractured basement reservoir becomes challenging. To address these challenges, an integrated data analysis was carried out. For the study, seismic facies was derived from acoustic impedance and a fracture network model was built by integrating the image logs with seismic derived fracture network. These two properties along with structural details of trap top were analyzed at each of the existing wells and compared with the well performance. The analysis successfully demystified the mysteries observed in several wells.

## Introduction

Deccan Trap basalt of Paleocene to Upper Cretaceous age forms the technical basement of the Cambay Basin (General Stratigraphy of Cambay Basin is shown in figure-1). It is overlain by a thick sedimentary succession of clastic reservoir rocks and shale barriers including Cambay shale as the major source rock (Raju, et al., 1971). The field of study lies in the north-eastern rising flank of the Broach depression of the Southern Cambay Basin. The trap structure shows a series of NNW-SSE trending normal faults almost parallel to one another. There are also some major transverse normal faults trending ENE-WSW to E-W cross-cutting the main longitudinal faults, resulting in a series of fault blocks and many fault closures within it.



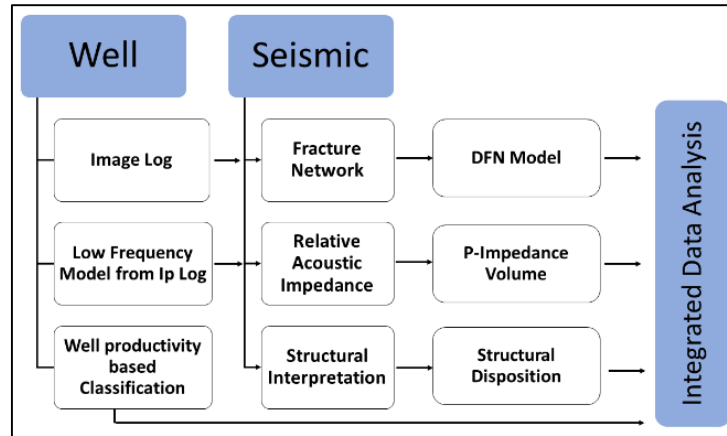


Fig-3. Workflow adopted for analysis

Using seismic data, 3D Acoustic impedance and variance/coherence attributes were obtained. Fractured/weathered zones of basaltic trap have lower acoustic impedance (referred to as seismic facies) than non-weathered trap, hence low impedance zones may be a potential reservoir. Using variance attribute, a 3-D fracture network (Ant-track) was generated. A Discrete Fracture Network (DFN) model was built by integrating the 3D-fracture network and image logs. Wells having significant production history were classified as Oil wells, wells that tested as oil but did not flow were classified as oil-Influx wells, and wells that were water bearing or non-fractured were classified as dry wells. The distribution of oil/oil-Influx/dry wells with the analyzed parameters was able to significantly discriminate between oil/oil-Influx wells from dry wells. Workflow adopted for analysis is shown in Figure-3.

## Well Data Analysis

Data from production logging in wells indicates that hydrocarbon production is predominantly from the upper fractured zones. It suggests that the oil migration might have happened through overlying Olpad or Anklawar formation. As the oil migrated to fractured basalt from overlying rock, the first non-permeable basaltic flow regime from the top of the trap would have restricted further downward migration of oil.

Image logs are extensively used for the identification of the fractured basement of the Cambay basin (Jamkhindkar, et al, 2013). Well logs data of 112 wells were analyzed. It was observed that image log (FMI), neutron, sonic and density logs were able to differentiate between fractured/non-fractured basaltic Trap. The caliper log was extensively referred to check the quality of log data. In the case of large casing or poor-quality data, the logs were rejected. Using image log (FMI), the natural fractures were picked in the basaltic trap and their corresponding dips are also shown in the image log of well-X (figure-4a). The rose diagram of natural fractures (fig-4b) clearly shows that the natural fractures are confined in two major directions, NNW and NNE in the vicinity of the borehole.

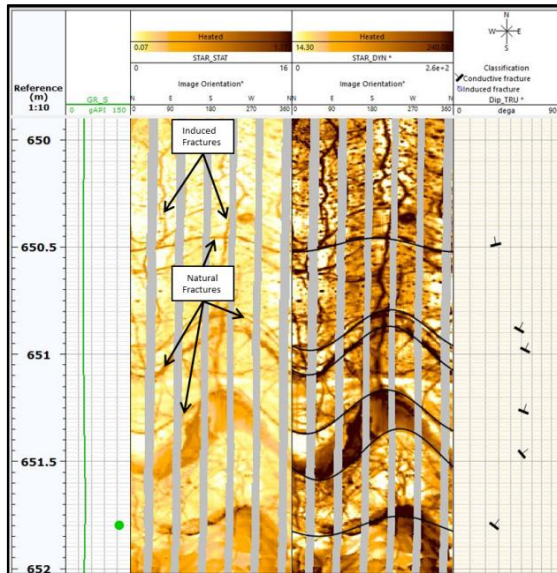


Fig-4a Image log showing static and dynamic.

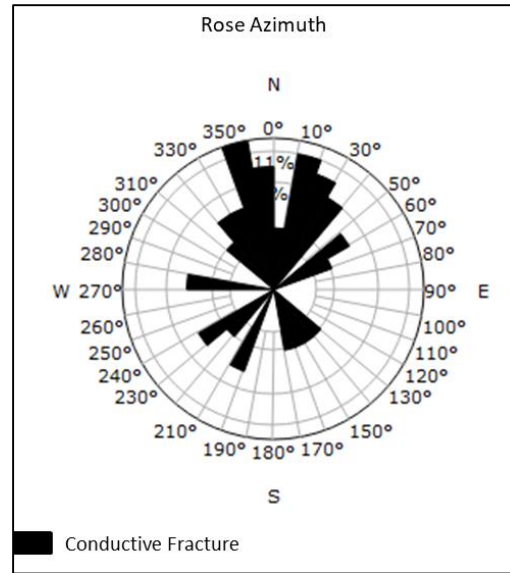


Fig-4b. Rose diagram of natural fractures.

In figure-4c, the Ant-Track derived fracture network (close to well-x) also shows the major faulting in NW and NE directions.

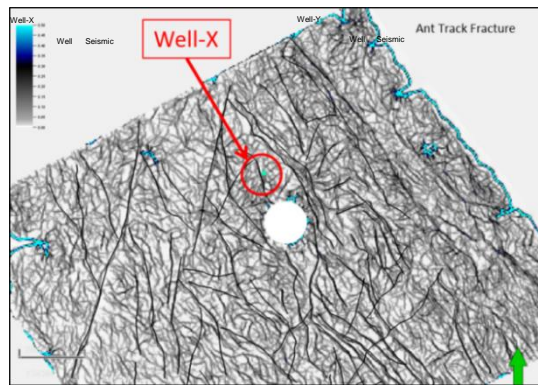


Fig-4c. Ant-track derived fault/fracture network

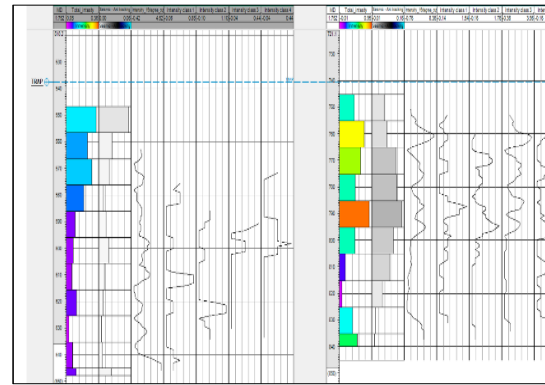


Fig-4d Up-scaled fracture intensity log with seismic derived fracture intensity.

Image/sonic log data were also utilized to compute fracture intensity. Based on image log interpretation, Trap zones having total fracture intensity more than 0.15 is considered as fractured. The total fracture intensity logs were up-scaled and compared with seismic derived fracture intensity. (Up-scaled fracture intensity logs of two wells along with seismic fracture intensity is shown in figure-4d). Figure-4d Up-scaled fracture intensity log (track-1 from left) with seismic derived fracture intensity (track-2 from left) shows a good correlation. Track-3 to 6 are directional fracture intensities.

Well data was also utilized for calculating P-Impedance using sonic and density log. Due to fracturing of the basaltic trap, the Density, as well as P-wave velocity of the trap, reduces significantly and it results in lowering in the P-impedance. The lower impedance values correspond to the fractured basement and higher values to the non-weathered basement rock. Logs filtered at seismic frequency bandwidth (6-60 Hz) shows that it can still capture low/high impedance contrast. Based on the filtered log data, it can be inferred that seismic-derived impedance may differentiate between fractured/weathered and non-weathered basaltic tarp.

### Structural Analysis of Trap Top

The analysis was carried out to evaluate the role of structure in the entrapment of hydrocarbon within the traps. A detailed structure map was generated by incorporating all the major/minor faults and horizon of the trap top. In the seismic section, all the well locations were analyzed for their structural disposition. First, all the wells having good fracture intensity were analyzed, and then it was extended to all the wells. A west to east seismic arbitrary line passing through five wells is shown in figure-5. The first two wells from the west do not form structural closure. Despite having good fracture intensity, they were found to be Dry/water-bearing. The third well from the west falls at the flank of very good structural closure, and have good fracture intensity but the well was found to have oil influx. The first two wells from the east, fall within very good structural closure, both have good fractures, and they are good oil producers. It suggests that wells having good structural disposition and fracture intensity are most likely to have hydrocarbon.

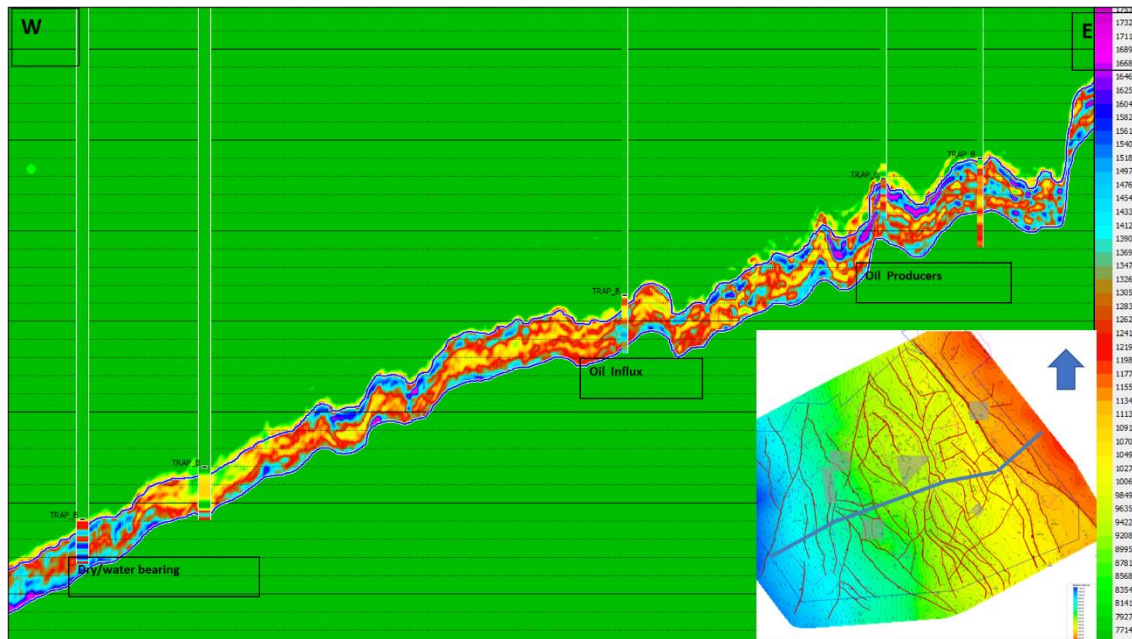


Fig-5. West to east arbitrary line (Ip) showing structural dispositions of wells.

The analysis demonstrated that structural disposition also plays a dominant role in hydrocarbon entrapment. It was observed that some water-bearing/dry wells had good structural disposition and fracture intensity, suggesting that good fracture and structure may not be enough to avoid dry wells.

## Seismic Facies Analysis

Model-based post-stack inversion was performed to obtain P-impedance ( $I_p$ ) volume. Fifteen wells, covering the entire field and two horizons were selected for building low-frequency model. A high cut filter 10/15 Hz was applied on the  $I_p$  log to build low-frequency model. Inversion analysis was carried out for all the wells having good sonic and density logs. (Inversion analysis for well-A is shown in figure-6). The inverted log below trap shows a good correlation with actual log data with minimal error. After achieving a good correlation and least error in the inversion analysis, the inversion was performed for the window between horizons Dadhar-60ms to Trap+60ms. The inverted P-impedance shows very good correlation with well-derived impedance. It is also observed that impedance range corresponding to 9000 KPa.s/m to 14000 KPa.s/m represents fractured zones and it is classified as seismic facies. Impedance ranging from 14000 KPa.s/m and above is classified as poor facies or non-weathered trap.

A map of the mean amplitude of P-impedance was extracted for the window from Trap top to

trap+20ms (figure-7). The low Impedance zones observed in the map (figure-7) correspond to the fractured trap. The highlighted area in the map having low impedance (seismic facies) is a horst-like structure bounded by intersecting faults causing intense fracturing. The majority of wells within the encircled area are oil producers and it is the most prolific zone of the field.

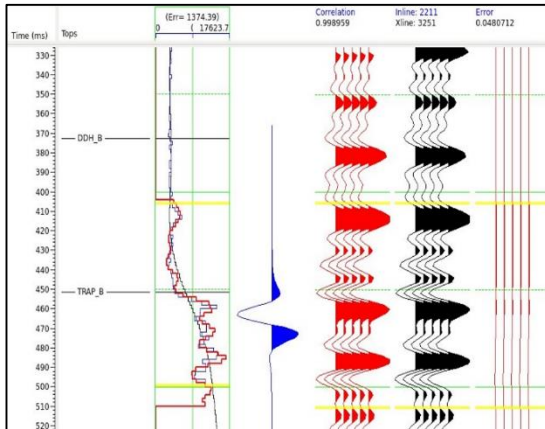


Fig-6. Inversion analysis at well-A.

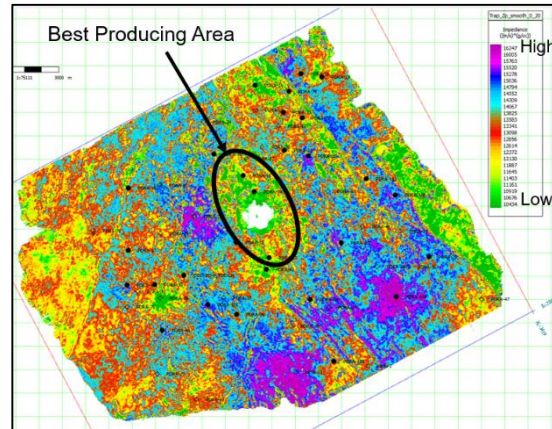


Fig-7. Mean amplitude of P-impedance for window Trap-Trap+20ms.

### Discrete Fracture Network Model

Seismic data was conditioned to enhance discontinuity and volume attributes such as variance and coherence were generated. 3D-Fracture Network (Ant-Track) volume was generated using variance attribute. Depth converted Ant-Track volume and up-scaled image logs were utilized to build the Discrete Fracture Network (DFN) model. The DFN and seismic facies have shown strong correlation i.e., a low impedance zone is equivalent to high fracture zone and vice versa. The lateral continuity was much more prominent in impedance than DFN.

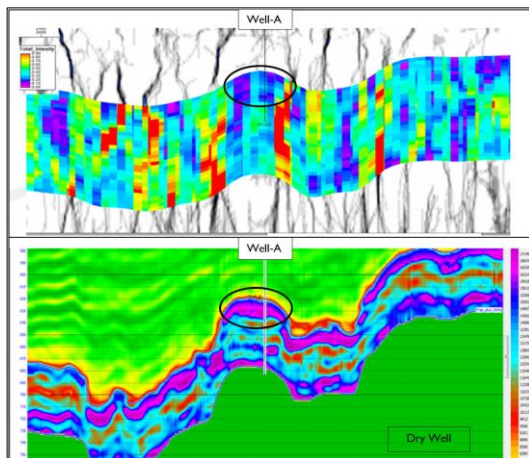


Fig-8. DFN model in depth (upper) and section in time (lower): High impedance corresponding to low fracture intensity at a dry well.

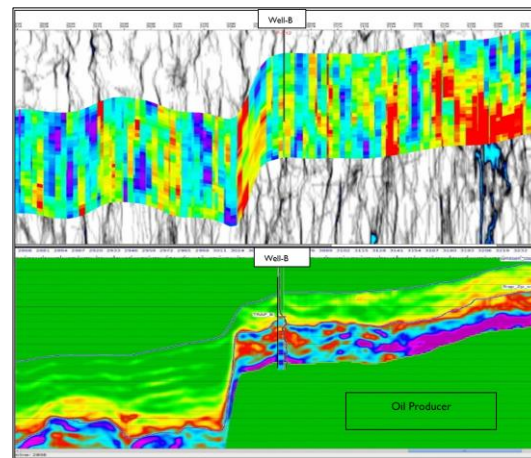


Fig-9. DFN model in depth (upper) and impedance section in time (lower): low impedance corresponding to high fracture intensity at a good oil producer from the trap.

A line passing through well-A, has good structure, poor seismic facies (high impedance) and low fracture intensity (as shown by DFN model) is a dry well (shown in figure-8). Another line passing through well-B has good structure, good seismic facies (low impedance) and high fracture intensity (as shown by DFN model) is a good oil producer (shown in figure-9). Fracture intensity greater than 0.15 was classified as fractured and less than 0.15 as non-fractured trap. The

fracture intensity, seismic impedance, and structural disposition of all the wells having good data quality were analyzed.

### Analysis of Seismic facies, DFN, and Structural Elements at wells

The observations from well data, structural elements, and seismic facies lead to the conclusion, that fractures in the basaltic trap are essential to form a reservoir, but it is not a sufficient condition for oil occurrences. This conclusion complicated the identification of sweet spots which, till now, depended primarily upon fracture intensity. To address the problem of identifying sweet spots all the data sets were analyzed altogether.

### Data Selection

Based on production history, wells are classified in three categories, namely; Oil wells, Oil-Influx wells and, Dry wells. Analysis of all the wells was attempted, considering production data vis-à-vis the presence of structural element, seismic facies, and fractures at the well location. Total 112 wells were analyzed and sorted by their properties and performance (shown in Table-1). Wells having poor log data were rejected. The bar graph distribution of properties for all three well categories is shown in Figure-10a.

Property/ Performance	Oil wells (52 Wells)	Oil Influx (31 wells)	Dry (29 wells)
<b>Structure</b>	41	18	9
<b>Facies</b>	46	17	17
<b>Fracture</b>	49	19	20

Table-1 Shows the presence of reservoir characteristics vs well performance.

### Probability Estimation

It is observed that fractures are present in the majority of wells (88 out of 112 or 79%), and it is no surprise as the criterion for identifying the sweet spot was primarily dependent on fracture intensity. Fractures are present in 49 oil wells (out of 88 fractured wells), which translates into the probability of oil wells with respect to all fractured wells to 56%. Similarly, the probability of oil wells with respect to total wells having seismic facies and structure element is 58% and 60% respectively.

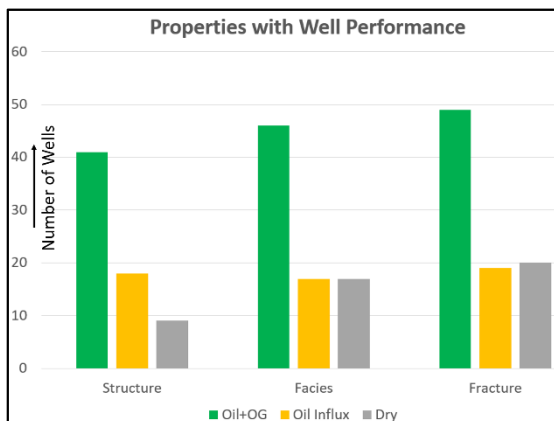


Fig-10a. Bar distribution of wells categories (Oil, Oil Influx, Dry) with respect to properties. In the histogram, Structure has lowest dry well. While wells having good seismic facies and fracture have similar number of oil influx and dry wells.

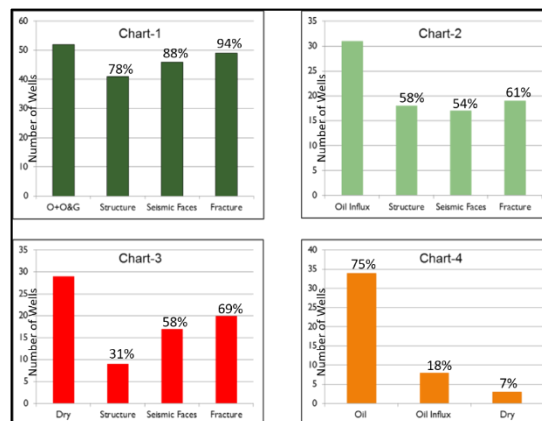


Fig-10b. Histogram of well performance and corresponding properties. From chart-1 to 3, the first bar is total number of wells (oil, oil- influx and dry category respectively) while next three bars are of wells having different properties. The chart-4 is the percentage of wells (Oil, Oil Influx, Dry)



## Histogram Analysis

Analysis of oil well category shows that strong fracturing is present in 94% of oil wells, and good seismic facies and structural disposition are present in 88% and 78% respectively (Histogram is shown in Chart-1 in figure-10b). In the case of the oil-influx well category; strong fracturing is present in 61% of wells, and good seismic facies and structural disposition are present in 54% and 58% respectively (Histogram is shown in Chart-2 in figure-10b). The dry well category analysis brings out the most puzzling results. It shows that strong fracturing is present in 69% of dry wells, and good seismic facies and structural disposition are present in 58% and 31% respectively (Histogram is shown in Chart-3 in figure-10b). It is evident from the dry well category analysis that fracture intensity, seismic facies (derived from low impedance), and structural element alone, are not sufficient for determining potential oil zones within traps.

To overcome this problem all the wells were sorted with respect to all three properties. The wells satisfying all three properties, namely; fracture, facies, and structure were worked out (total 45 wells). These 45 wells are then analyzed with respect to their production performance. The distribution (Histogram is shown in chart-4 in figure-10b) shows that there are 34 oil wells, 8 oil-influx wells, and only 3 dry wells which have all three properties. Implying that if all three properties are satisfied the likelihood of having dry wells is lowest (7%) and the chances of hydrocarbon occurrence is highest (75%).

## Result and Conclusion

Integrated data analysis was carried out with all the available data sets. The emphasis was given on analyzing the effect of all the parameters (fracture, facies, structure) on the production performance of the well. Before the study, wells were drilled by identifying good fracture intensity zones. But it was observed that several water-bearing/dry wells (69%) also had strong fracture intensity. This observation leads to the principal outcome of the study that the fracturing in the basement is necessary, but not sufficient condition for oil occurrence. The study has shown that structural disposition also plays a prominent role in hydrocarbon entrapment. Seismic facies (low impedance) which is complementary to fracture network, helps in analyzing the lateral distribution of fractured basement. The analysis successfully demonstrates that if a given location satisfies all three properties (good fracture, seismic facies, and Structural disposition), then the probability of having a dry well is the lowest (7%) and the probability of the location having an oil well is highest (75%). The study was utilized to identify new locations having all three parameters and subsequently several identified development locations were successfully proposed. This methodology should be incorporated in other fractured basement reservoirs for the identification of sweet spots.

## Acknowledgment

The authors are thankful to Oil and natural gas Corporation Ltd. for granting permission to publish the work. The Discrete Fracture Modelling was carried out by COD-Basement Group, Mumbai. The authors sincerely acknowledge the valuable inputs obtained from COD-Basement Group, Mumbai and Western Onshore Basin, Baroda, ONGC. The authors are grateful to the Director Exploration for providing us the opportunity to publish the article. The authors are also grateful to Head-IRS, Ahmedabad for his support and encouragement.





*Views expressed in the paper are Author(s) opinions and not of the ONGC*

## References

Sanders C. A. E., Fullarton L., Calvert S.; Modelling fracture systems in extensional crystalline basement. Geological Society, London, Special Publications, Jan, 2003.

Raju, A.T.R., Chaube, A.N. & Chowdhary, L.R.; Deccan Trap and the geologic framework of the Cambay basin. Bull Volcanol 35, 521–538 (1971)

Deepa, J. Nagaraju, Binod Chetia, Tandon Rajeev, Chaudhuary, P. K., and Bhardwaj A.; Integrated study of a fractured granitic basement reservoir with connectivity analysis and identification of sweet spots: Cauvery Basin, India. The Leading Edge, April-19.

Jamkhindikar A., Jain Mukesh, Mohanty S.N.; Hydrocarbon Prospectivity of Deccan Trap in Northern Cambay Basin. P167, SPG India-2013.

Goyal Uma, Chitnis S. N. and Ray B. B.; Challenges in identifying hydrocarbon potential in fractured Basement in Mumbai High field. P286, SPG India-2013.

Singh Nepal; Fractured Basement Reservoir Characterization in Barmer Basin. SPE-185419-MS, 2017.

Raghuvanshi H., Agarwal B., Sharma R. K.; Analyzing the Multi-Component 3D-3C data of Padra Area to Understand the Fracture Geometry of the Basement. Unpublished ONGC Internal Report, 2019.

Suardana M.; Identification of Fractured Basement Reservoir Using Integrated Well Data and Seismic Attributes: Case Study at Ruby Field, Northwest Java Basin. Search and Discovery Article, 2013.